Plant and Cell Physiology Advance Access published October 6, 2009

Running title: AtRPA70a for DNA repair and telomere maintenance

Corresponding Author: Katsunori Tamura
Institute of Molecular and Cellular Biosciences, University of Tokyo, 1-1-1 Yayoi, Bunkyo-ku, Tokyo 113-0032, Japan. Tel.: +81-3-5841-7826. Fax: +81-3-5841-8476.
E-mail: ktamura@ iam.u-tokyo.ac.jp

Subject Areas: environmental and stress responses

Number of black and white figures: 2
Color figures: 3
Number of table: 1

Arabidopsis replication protein A 70a is required for DNA damage response and telomere length homeostasis

Yoshiyuki Takashi, Yuki Kobayashi, Kan Tanaka, and Katsunori Tamura

Institute of Molecular and Cellular Biosciences, University of Tokyo, 1-1-1 Yayoi, Bunkyo-ku, Tokyo 113-0032, Japan

Abbreviations

AD, activation domain; 3-AT, 3-amino-1',2',3'-triazole; BD, DNA-Binding domain; CBB, Coomassie brilliant blue; DIG, digoxigenin; HA, hemagglutinin; MS, Murashige-Skoog; OB-fold, oligonucleotide-binding fold; RT–PCR, reverse transcription–PCR; UTR, untranslated region.

Abstract

Replication protein A1 (RPA1/RPA70) forms a heterotrimeric complex together with RPA2/RPA32 and RPA3/RPA14 subunits, that plays essential roles in various DNA metabolisms including replication, repair, recombination and telomere maintenance. Compared to RPA70 in yeast and mammals, limited information is available on the factor in plants. In this study, we analyzed functions of AtRPA70a, which is most similar to human RPA70 among four paralogs in *Arabidopsis thaliana*. RNA blot analysis showed that *AtRPA70a* expresses ubiquitously in plant organs containing differentiated and meristematic tissues, while the expression was upregulated in response to DNA damage stress. Yeast two-hybrid and co-immunoprecipitation analyses showed that AtRPA70a interacted preferentially with *Arabidopsis* RPA32a, one of two paralogs. Inactivation of *AtRPA70a* by T-DNA insertion did not affect the growth under normal conditions, but resulted in increased sensitivity to genotoxic agents such as methylmethane sulfonate, bleomycin, and hydroxyurea. Terminal restriction fragment analysis revealed that telomere lengths in *AtRPA70a*-deficient line were significantly larger than wild type, whereas those in the mutant expressing antisense *AtTERT* (telomerase catalytic subunit gene) were shortened during generations. These results demonstrate that AtRPA70a is involved in repair of double-strand DNA breaks and possibly contributes to telomerase-dependent telomere length regulation.

Key words: *Arabidopsis thaliana*, cell cycle checkpoint, DNA repair, telomere maintenance.

Introduction

Single-stranded DNA (ssDNA) is the biologically important intermediate in various DNA metabolic pathways formed in all living cells. It is, therefore, critical that ssDNA is protected from unwanted attack by nucleases and that its unwound state is maintained for important DNA metabolic reactions and the assembly of various related biological apparatuses. Replication protein A (RPA), the conserved eukaryotic ssDNA binding protein, is a heterotrimeric complex composed of three tightly associated subunits of 70-, 32-, and 14-kDa (referred as to RPA70, RPA32, and RPA14, respectively) (Iftode et al., 1999; Wold, 1997). The complex was originally isolated as a factor essential for *in vitro* DNA replication of simian virus 40 (SV40) (Bullock, 1997; Stenlund, 2003). Consistent with the importance of ssDNA formation, RPA is required for almost all aspects of cellular DNA metabolism such as DNA replication, recombination, DNA damage checkpoints, and all major types of DNA repair including nucleotide excision, base excision, mismatch, and double-strand break repairs, also in regulation of transcription (Wold, 1997). The common feature of all of these DNA processing is that each has ssDNA intermediates that must be recognized and processed appropriately. RPA interacts with ssDNA through own DNA-binding domains (DBDs) and with a number of proteins involved in these processes, and appears to actively coordinate the sequential assembly and disassembly of DNA processing proteins on ssDNA (Fanning et al., 2006). The ability of RPA to guide DNA processing pathways depends in large part on RPA interactions with other proteins in each pathway (Fanning et al., 2006).

The RPA70 subunit represents the most extensively characterized component of the RPA complex. This subunit is involved in DNA-binding (Kim et al., 1994) and is implicated in the majority of the described protein interactions (Wold, 1997). Biochemical studies have delineated three distinct domains of the protein. The N-terminal domain (aa 1–170) that is involved in RPA-protein interactions, a central DNA binding domain (aa 170–450) and C-terminal domain (aa 450–616) required for binding the other two subunits (Bochkareva et al., 2001). Zinc binding in the C-terminal OB-fold of RPA70 is important for RPA structural stability and ssDNA binding (Bochkareva et al., 2000). The largest protein interaction module of RPA70 spans domains 70A and B (residues 168–308/327) and is reported to interact with the primase subunits of DNA polymerase alpha-primase, the SV40 T antigen helicase and the RecQ family Werner and Bloom Syndrome helicases (Braun et al., 1997; Doherty et al., 2005). There is evidence that these interactions have physiological importance. For example, RPA stimulated the DNA unwinding activity of Werner helicase fragments capable of binding to RPA (Doherty et al., 2005). The interaction of Rad52 with RPA in homologous recombination has been investigated in detail [for a review see (Cahill et al., 2006)]. In yeast, Rad52 association with RPA plays an important role in mediating Rad51 assembly on RPA-coated ssDNA (Song and Sung, 2000; Sugiyama and Kowalczykowski, 2002; Symington, 2002). A number of other DNA damage signaling and processing proteins have been shown to interact directly or indirectly with RPA70; Rad17 clamp loading complex (Zou et al., 2003), Rad9 clamp subunit (Wu et al., 2005), ATR-interacting protein (ATRIP) (Zou and Elledge, 2003; Ball et al., 2005; Namiki and Zou, 2006), 53BP1 (Yoo et al., 2005), BRCA2 (Wong et al., 2003), Mre11–Rad50–Nbs1 (Robison et al., 2004) and nucleolin (Daniely and Borowiec, 2000; Kim et al., 2005).

In addition to the above-mentioned roles in DNA metabolism, recent studies have shown critical roles for RPA in maintenance of telomeres. It was reported that mutations in the genes encoding *Schizosaccharomyces pombe* and *Saccharomyces cerevisiae* RFA-1 (replication factor A-1; RPA-1 homologue in yeast) respectively caused defects in telomere length regulation (Ono et al., 2003) and a reduction in telomere length (Smith et al.,

2000). It was shown that budding yeast RPA is present at the telomeres, with a maximal association in the S phase of cell cycle, and that RFA-2, an RPA-2 homologue in yeast, facilitates the access of telomerase to chromosomal ends by direct binding to Est1p, a subunit of telomerase holoenzyme, to regulate the telomerase-mediated lengthening of telomeres (Schramke et al., 2004). Human RPA-1 (hRPA-1), similarly to telomeric G-rich single-strand DNA binding proteins such as human POT1 (Protection of Telomeres 1) and ciliate TEBP (Telomere End-Binding Protein), modulates the unfolding of intramolecular G-quadruplex formed by the single-stranded telomeric oligonucleotides *in vitro*, allowing telomere elongation by telomerase (Zaug et al., 2005; Salas et al., 2006). Moreover, hRPA was shown to be a component of constitutes a complex with WRN (Werner syndrome) and BLM (Bloom syndrome) helicases, that actively unwinds long telomeric duplex regions, suggesting that all these proteins function in a common pathway at telomere ends (Opresko et al., 2002). More recently, RPA has been shown to control the telomerase-independent mechanism for maintaining telomeric repeats that relies on homologous recombination (Grandin and Charbonneau, 2007).

In contrast to RPA in yeast and animals, little is known about DNA metabolism mediated by RPA in plants. By using biochemical techniques, an RPA protein complex was firstly isolated from tobacco by binding and elution from single-stranded DNA and was shown to induce DNA polymerase activity (Garcia-Maya and Buck, 1997). It was shown that most of animals and yeasts possess single gene for each of RPA subunits except for the existence of two RPA32 paralogs in human. On the contrary, rice (*Oryza sativa* L.) and *Arabidopsis* carry muliple paralogs for each of RPA subuits (van der Knaap et al., 1997; Ishibashi et al., 2001; Xia et al., 2006). Interestingly, it was suggested that such paralogous RPA subunits could be divided into two types based on their expression manners and roles in DNA metabolism (Ishibashi et al., 2001; 2005). Despite of its possible importance in DNA transactions, cellular function of *Arabidopsis* RPA70a (AtRPA70a), which is most similar to human RPA70 among four paralogs in this organism, remains unclear. Here, we provide evidence that AtRPA70a plays an essential role in DNA damage response as well as in telomere length regulation through investigating cellular consequences of functional deficiency in this factor.

Results

Structural comparison of four *Arabidopsis* RPA70 paralogs

Ishibashi et al. (2005) previously reported that there are two paralogs for RPA70 subunit, AtRPA70a (At2g06510) and AtRPA70b (At5g61000) in *A. thaliana*. In addition, Xia et al. (2005) described that *Arabidopsis* possesses four RPA1, which were referred to as AtRPA70a (At2g06510), AtRPA70b (At5g08020), AtRPA70c (At5g45400), and AtRPA70d (At5g61000). Since the names of paralogs were confused between the two reports, we employed the latter naming. The TBALSTN search with the GenBank *Arabidopsis* database (http://www.arabidopsis.org/blast) against human RPA1 (HsRPA1) indicated the E-values of 9e-103 for AtRPA70a, 9e-92 for AtRPA70c, 3e-82 for AtRPA70d, and 7e-79 for AtRPA70b (Fig. 1A). The domain search with Pfam database (http://pfam.sanger.ac.uk/) showed that all the four AtRPA70 paralogs contain three characteristic domains; N-terminal domain of replication protein A at the N-terminal region, the anti-codon binding domain of lysyl, aspartyl, and asparaginyl -tRNA synthetases known as OB-fold nucleic acid binding domain at the central region, and C-terminal domain of replication factor-A at the C-terminal region (Fig. 1A). When the amino acid sequence of the entire region were compared among *Arabidopsis* RPA70 paralogs and

HsRPA1, AtRPA70a showed 33.08, 40.72, 32.93 and 36.53% sequence identities with AtRPA70b, AtRPA70c, AtRPA70d and HsRPA1, respectively; AtRPA70b showed 25.84, 81.30 and 31.50% sequence identities with AtRPA70c, AtRPA70d and HsRPA1, respectively; AtRPA70c showed 26.67 and 29.30% sequence identities with AtRPA70d and HsRPA1, respectively; AtRPA70d showed 31.97% sequence identities with HsRPA1.

To investigate the phylogenetic relationship among RPA70 homologues in diverse eukaryotic organisms including the AtRPA70 paralogs, an unrooted tree was drawn based on the alignment using MEGA (Molecular Evolutionary Genetics Analysis) Software Version 4.0 (Fig. 1B). The tree showed that, similar to the situation in rice, which was previously reported to possess two different types of RPA70 (Ishibashi et al., 2001; 2005), *Arabidopsis* RPA70 paralogs were divided into two groups; one comprised AtRPA70a and AtRPA70c, whereas the other consisted of AtRPA70b and AtRPA70d (Fig. 1B). OsRPA1 is an RPA70 homologue, which was isolated from deepwater rice (*Oryza sativa* cv. Pin Gaew 56), and is closely related to OsRPA70b from another rice cultivar Nipponbare (van der Knaap et al. 1997; Ishibashi et al. 2001). We also compared the amino acid sequence corresponding to each of three domains; similarity was higher between members within each group than between another group members (Table 1).

AtRPA70a expression is ubiquitously in plant organs and upregulated by genotoxic stress

Because of the highest E-value (9e-103) for AtRPA70a against HsRP-A1 (Fig. 1A), we focused on the function of AtRPA70a in plant growth and development as well as in response to genotoxic stress. We investigated expression profile of *AtRPA70a* in various *Arabidopsis* organs, seedlings and suspension-cultured cells. RNA blot analysis using total RNA extracted from each organ of 6-week-old plants showed that almost equal levels of steady state mRNA were detected in rosette leaves, stalks, flower buds and roots, indicating ubiquitous expression of *AtRPA70a* in plant organs (Fig. 2A). In addition, steady state mRNA level of the gene in one-week-old seedlings was similar to those in mature plant organs, suggesting that the gene expression might not fluctuate during plant development (Fig. 2A). We next examined whether DNA damage stress affect the expression of *AtRPA70a*. RNA blot analysis showed that the transcript levels of the gene were increased within 30 min in seedlings treated with methyl methane sulfonate (MMS) and bleomycin, which are known to induce double strand DNA breaks (DSBs) (Fig. 2B). These results suggested that the expression of *AtRPA70a* is regulated in response to genotoxic stress at the transcriptional level.

AtRPA70a interacted more preferentially with AtRPA32a than AtRPA32b

In RPA complex composed of RPA70, RPA 32 and RPA14 subunits, RPA70 directly interacts with RPA32. The TBLASTN search of RPA32 on *Arabidopsis* genome revealed two paralogs AtRPA32a (At2g24490) and AtRPA32b (At3g02920) in this organism. In rice, specific interactions have been shown between paralogs of RPA70 and RPA32 (Ishibashi et al. 2005). To examine whether AtRPA70a interacts preferentially either with AtRPA32a or AtRPA32b, yeast two-hybrid analysis was performed using the full-length coding region of the *RPA32* genes. In case of using activation domain fused to AtRPA32b, growth of yeast cells was severely inhibited; therefore, we analyzed protein-protein interactions using combinations between binding domain fused to AtRPA32a or AtRPA32b and activation domain fused to AtRAP70a. Growth assay of yeast cells showed that AtRPA70a bound more strongly to AtRPA32a than to AtPRA32b on a 3-AT-containing SD medium deficient in leucine, tryptophan, uracil, histidine and adenine, indicating preferential interaction of AtRPA70a with

AtRPA32a (Fig. 3A). This was verified by reporter assay of β-galactosidase activity; the enzyme activity in combination of AtRPA70a with AtRPA32a was about 10-fold higher than that with AtRPA32b (Fig. 3B). The preferential interaction was also confirmed by co-immunoprecipitation analysis; HA-tagged AtRPA70a bound to myc-tagged AtRPA32a, but not to myc-tagged AtRPA32b (Fig. 3C).

Defects in *AtRPA70a* resulted in increased sensitivity to genotoxic stress.

To examine the roles of AtRPA70a in growth and development as well as in response to DNA damage stress, we analyzed a T-DNA insertion mutant (SALK_017580), in which the T-DNA is located at the third exon (Fig. 4A). After self-fertilization for three times, a homozygous T-DNA insertion line was identified by the PCR-based genotyping (Fig. 4B). Since the transcript of *AtRPA70a* could not be detected from rosette leaves of the mutant by RT-PCR (Fig. 4C), the line was considered to be a null mutant. Neither growth abnormality nor retardation was detected in the *atrpa70a* plant grown under normal long-day conditions, suggesting that AtRPA70a is not essential under such normal growth conditions. Ishibashi et al. (2005) previously reported that screening of homozygous T-DNA insertion mutant of *AtRPA70a* was failed. The discrepancy might be due to technical differences in screening of homozygous T-DNA insertion lines.

When one-week-old seedlings of the *atrpa70a* mutant were transplanted onto MS medium containing various concentration of DNA damaging agents such as MMS and bleomycin, they exhibited growth arrest and necrotic death on MS plate containing MMS at the concentration of 0.005 % as well as bleomycin at 10 μg/ml, both of which caused negligible effects on the growth of wild type seedlings (Fig. 4D). Significant inhibition of root growth in the mutant line was observed at such concentrations of the DNA damaging agents (Fig. 4E). The phenotypes of *atrpa70a* mutant were complemented almost completely by introduction of genomic *AtRPA70a* transgene into the mutant (data not shown). These results suggest that AtRPA70a is responsible for DNA damage response, or is required for the repair of DSBs induced by MMS and bleomycin. In addition, *atrpa70a* seedlings showed increased sensitivity to hydroxyurea (HU), the specific inhibitor of ribonucleotide reductase, at the concentration of 10 μg/ml (Fig. 4D and 4E).

Defects in *AtRPA70a* led to telomere lengthening

In yeast and mammals, RPA is involved in telomere length regulation (Cohen et at., 2004; Smith et al., 2000; Schramke et al., 2004). To investigate roles of AtRPA70a in telomere length homeostasis, we analyzed telomere lengths in rosette leaves of *atrpa70a* by means of the terminal restriction fragment (TRF) assay. Results showed that the mean telomere length of *atrpa70a* was significantly longer than that of wild type plant (Fig. 5, lanes 2 and 3, compared to lanes 1 and 8), indicating that AtRPA70a negatively contributes to telomere length regulation. The results were confirmed by introduction of genomic *AtRPA70a* into *atrpa70a* mutant, which showed reversion of telomere lengths to nearly normal size for wild type Col-0 plants (Fig. 5, lanes 11 and 12, compared to lanes 8-10). To examine whether the function of AtRPA70a is associated with telomerase activity, we generated an *atrpa70a attert* double mutant line by crossing between a pistil of *atrpa70a* and a stamen of *attert* (4th generation; G4), which had been deficient in telomerase reverse transcriptase gene by T-DNA insertion. In the *atrpa70a tert* (G4) double mutant, telomere lengths were shortened within a generation (Fig. 5, lanes 4 and 5, compared to lanes 2 and 3). In addition, suppression of *AtTERT* gene expression in *atrpa70a* plants by antisense RNA technique resulted in reduced telomere lengths with diverse extents depending on the independent lines

(Fig. 5, lanes 14-16). Thus, these results suggest that AtRPA70 plays a role in the telomerase-dependent telomere length homeostasis.

Discussion

The functions of RPA70 in DNA processing have been well characterized in yeasts and human (Wold et al., 1998). In the present study, we characterized *Arabidopsis* RPA70a, which is most similar to human RPA70 among four paralogs existing in this plant species. Our data showing ubiquitous expression of *AtRPA70a* implicate that this factor is not directly linked to mitotic activity, but rather might contribute to repair of DNA damages occurred in somatic cells. Consistent with this idea, the expression of *AtRPA70a* was upregulated by genotoxic agents, which induce DSB. It has been demonstrated that RPA is involved in both of the major DSB repair pathways including the homologous recombination (HR) and non-homologous end joining (NHEJ), despite the role of RPA in NHEJ is not well defined (Binz et al., 2004). Considering that DSB in somatic plant cells are preferentially repaired by NHEJ rather than HR (Pacher et al., 2007), it is likely that AtRPA70a plays a role in the NHEJ-mediated DSB repair pathway.

Our results showed that *atrpa70a*-deficient mutant exhibited elevated sensitivity to hydroxyurea, a specific inhibitor of ribonucleotide reductase, which leads to replication fork stalling due to depletion of deoxyribonucleotide substrates (Sogo et al., 2002). It has been known that RPA is also required for activation of cell cycle checkpoint pathway in response to replication blocks. In budding yeast, certain mutations in *RPA70* caused altered response to replication stress (Longhese et al., 1996). Evidence has shown that the human RPA binds to ssDNA generated at the site of stalled replication folks, and that the RPA-ssDNA complex is recognized by ATRIP, followed by activation of the checkpoint kinase Chk1 (the initiation of checkpoint signaling) (Zou and Elledge, 2003). Moreover, it was reported that RPA in budding yeast is required for loading of Rad1-Hus1-Rad9 onto ssDNA by the Rad17–Rfc2-5 complex, both of which complexes are necessary for a normal cellular checkpoint response, indicating that RPA is required for checkpoint activation by the Rad17 pathway (Zou et al., 2003). Although the DNA replication checkpoint pathway in plant cells has not yet been elucidated, our results suggest a role for *Arabidopsis* RPA70a in the S-phase checkpoint activation pathway following exposure to DNA replication stress.

Unlike yeasts and mammals, except that human carries an another gene for RPA32, which was referred to as *RPA4* (Keshav et al., 1995), *Arabidopsis* and rice possess multiple genes for each RPA subunit. It was suggested on the basis of amino acid sequence similarity and yeast two-hybrid analysis that the *Arabidopsis* four RPA70 paralogs could be divided into two groups either of which likely has a preferable interaction partner of AtRPA32, similar to the situation in which RPA70 and RPA32 paralogs in rice were grouped into two types (Ishibashi et al., 2005). A phylogenetic tree of the RPA70 proteins clearly indicated that paralogs split up into two distinct groups. The classification is further substantiated by the gene expression profiles. We envision two possible significances for the presence of multiple genes for RPA subunits. One interpretation is that such a multigene family in DNA repair pathway might be responsible for greater DNA repair capacity, which had been evolved in higher plants. On the other hand, it has been postulated that the multiplicity of genes for DNA repair and recombination could be conceivably due to the transfer of genes from the organellar genomes to the nucleus, which are indispensable for maintenance of genome integrity in each organelle (Tuteja et al., 2001).

In addition to its multiple roles in DNA transaction, RPA has recently been shown to be required for telomere maintenance (Viscardi et al., 2005; Verdun and Karlseder, 2006). Our data showed that disruption of

AtRPA70a caused significant telomere lengthening, suggesting that *Arabidopsis* RPA negatively regulates the telomere length. Previous reports showed that *S. pombe rad11-D223Y* mutation (a miss-sense allele of *Rpa70*) caused telomere shortening (Ono et al., 2003), wherease *S. cerevisiae rfa1-D228Y* mutation, which corresponds to the *S. pombe rad11-D223Y*, didn't influence telomere lengths (Smith et al., 2000). Together, these findings implicate distinct roles in telomere maintenance for the RPA70 subunit in different organisms, similar to the situations for several *Arabidopsis* factors including KU70/KU80 (Riha et al., 2001; Gallego et al., 2002), MRE11 (Bundock and Hooykaas, 2002) and RAD50 (Gallego and White, 2001), which play an opposite role in telomere length regulation compared to the counterparts in yeast and mammals. We also showed that AtRPA70a contributes to telomerase-dependent telomere length homeostasis and probably AtRPA70a coordinated telomere lengths with other telomere-related proteins in this organism. Evidence showed that RPA in budding yeast facilitates the loading of Est1, a cell cycle–regulated activator of telomerase, onto telomeres (Schramke et al., 2004). Although EST1 ortholog has not been identified so far from plants, it is possible that RPA70 may play an important role in regulation of telomerase action in *Arabidopsis*. Meanwhile, in human cells and in fungi, telomere length can be maintained not only by telomerase activity but also by recombination-based mechanisms, referred to as ALT (alternative lengthening of telomeres) in human cells and as the survivor pathway in yeast (reviewed in Lundblad, 2002; Henson et al., 2003). Since the telomere lengths shortened slowly in the double mutant defective in *atrpa70a* and *attert*, as was observed in the *attert* single mutant (Fitzgerald et al., 1999), it is unlikely that AtRPA70a is involved in the alternative telomere maintenance mechanism. Further studies on functional features for AtRPA70a at telomeres, including its association with other telomeric proteins and regulation of telomerase activity will allow us to understand the plant specific-mechanism of telomere maintenance in more detail.

Materials and Methods

Plant materials, growth conditions, and assay for sensitivity to genotoxic stress.

A. thaliana (ecotype Columbia) seeds were sown directly onto Jiffy-7 peat pellets (AS Jiffy Product, Oslo, Norway) or surface-sterilized seeds were sown onto Murashige-Skoog (MS) plates, and plants were grown in an environmental growth chamber (Tomy, Tokyo, Japan) at 22 °C under continuous white light or under long-day (14 h light/10 h dark) conditions. Suspension cultured cells of *A. thaliana* (T87 line) were maintained in MS medium on a rotary shaker at 100 rpm at 22 °C under continuous white light, and subcultured once a week. T-DNA insertion line (SALK_017580) for *Atrpa70a* was obtained from the *Arabidopsis* Biological Resource Center (ABRC; Ohio State University, Columbus, OH). For assay of plant sensitivity to genotoxic treatments, one-week-old *Arabidopsis* seedlings were transplanted to solid MS media containing various concentrations of methylmethane sulfonate (MMS), bleomycin or hydroxyurea (HU). The seedlings were further grown at 22 °C under LD (16h-ligth/8h-dark) conditions, and sensitivity to genotoxic agents was assessed after 10 days of incubation.

Molecular cloning and sequence analysis.

General molecular biological techniques were performed according to standard protocols (Sambrook et al., 1989). Total RNA was extracted from plant materials using an RNeasy Plant Mini kit (Qiagen, Tokyo, Japan) and

complementary DNA was synthesized from the resulting RNA with the use of a ReverTra Ace Kit (Toyobo, Tokyo, Japan). Nucleotide sequences were determined by the Big-Dye terminator method with the use of an Applied Biosystems model 373S DNA sequencer (Perkin-Elmer, Chiba, Japan). Domain prediction was performed by Pfam search program (http://www.sanger.ac.uk/Software/Pfam/). Preliminary multiple sequence alignments were carried out by using CLUSTAL W program (Thompson et al., 1994), and phylogenic tree was constructed by the Neighbor-Joining (NJ) method using MEGA (Molecular Evolutionary Genetics Analysis) Software Version 4.0 (Tamura et al., 2007). The reliability of interior branches was assessed with 1,000 bootstrap resamplings by using Jones, Taylor, and Thorton (JTT) model for amino acid sequences and gamma parameters.

Gene expression analysis.

Total RNA was extracted from major organs of mature *Arabidopsis* plants, including roots, rosette leaves, stalks, bract leaves and flowers, as well as from suspension cultured cells using an RNeasy Plant Mini Kit (Qiagen). RNA blot analysis was carried out as previously described (Tamura et al., 2002). To prepare specific *AtRPA70a* probe, 3'UTR region was amplified by reverse transcription (RT) and polymerase chain reaction (PCR) using a ReverTra Ace Kit and the following oligonucleotide primers; RPA70a_F3'UTR (5'-GTTCGTTCTAGGTATTACAGTGAG-3') and RPA70a_R3'UTR (5'-TGATTCCGGAGATAGCTGAAGCTG-3'). The amplified fragment was cloned in pSPT18, and used for prepare DIG-labeled RNA probe (Roche, Indianapolis, IN, USA). For detection of *AtRPA70a* transcript, RT-PCR was carried out with the use of 1 μg total RNA as template in 20 μl reaction mixtures, reverse transcription was done at 42 °C for 20 min. Enzymes were inactivated with heat at 99 °C for 5 min. Polyubiquitine conjugating gene (*AtUBQ1*) was also amplified as the internal control with the primers AtUBQ-f (5'-CAATGTCAAGGCCAAGATCCA-3') and AtUBQ-r (5'-CAGTTGACAGCTCTTGGGTGA-3'). Amplified DNA fragments were fractionated by 1 % agarose gel electrophoresis, stained with ethidium bromide and detected under transiluminator.

Yeast two-hybrid analysis.

Protein-protein interactions were analyzed by yeast two-hybrid (Y2H) method (Fields and Sternglanz, 1994) using a BD Matchmaker Two-hybrid System 3 (Clontech, Palo Alto, CA, USA). The full-length coding region of *AtRPA70a* cDNA was amplified by RT-PCR with the following primers: RPA70a-F (5'-CAACATATGATGCCGGTGAGTTTGACTCCG-3'; *Nde*I site is underlined) and RPA70a-R (5'-GGATCGATCCTTACGAGCAAATCAAGCATG-3'; *Cla*I site is underlined). The amplified fragment of *AtRPA70a* was digested with *Nde*I and *Cla*I, and cloned into pGADT7 to generate a plasmid containing *AtRPA70a* fused to the activation domain of Gal4 (pAD-AtRPA70a). The full-length coding regions of *AtRPA32a* and *AtRPA32b* (accession numbers NM111162 and BT005433, respectively) were also amplified by RT-PCR with the following primers: RPA32a-F (5'-CCGAATTCATGTACGGAGGCGATTTTGACG-3', *Eco*RI site is underlined) and RPA32a-R (5'-CTGGATCCTCAAGCGTTAGCAGTCGATTTG-3', *Bam*HI site is underlined) for *AtRPA32a*, and RPA32b-F (5'-GGGAATTCATGTTCTCCAGCAGCCAATTCG-3'; *Eco*RI site is underlined) and RPA32b-R (5'-TTGGATCCCAAAGCTCCACGTGCTTGAAG-3'; *Bam*HI site is underlined) for *AtRPA32b*, respectively. The amplified fragment of *AtRPA32a* and *AtRPA32b* were digested with

*Eco*RI and *Bam*HI, and cloned into pGBKT7 to generate plasmid encoding *AtRPA32a* and *AtRPA32b* fused to the DNA-Binding domain of Gal4 (pBD-AtRPA32a and pBD-AtRPA32b, respectively). After transformation of *Saccharomyces cerevisiae* strains AH109 (MATa) and Y187 (MATα) with pBD-AtRPA32a or pBD-AtRPA32b, and with pAD-AtRPA70a, respectively, the transformants were mated, and subsequent growth was examined on complete supplemental medium (SD; Clontech) containing 10 mM 3-amino-1',2',3'-triazole (3-AT) but without leucine, tryptophan, uracil, histidine and adenine. For quantitative analysis of Y2H interactions, the liquid β-galactosidase assay was performed with *O*-nitrophenyl-β-D-galactopyranoside (ONPG) as the substrate according to the manufacturer's instructions.

Co-immunoprecipitation assay.

Immunoprecipitation and immunoblotting experiments were performed essentially as described (Wu et al., 2005). Briefly, the yeast cells used in the two-hybrid analysis were homogenized and solubilized in TS buffer [50 mM Tris-HCl (pH 8.0), 175 mM NaCl, 0.05% [v/v] Triton-X 100, 1 units of complete proteinase inhibitors (Roche)], followed by centrifugation at 17,400 *g* for 10 min at 4°C to remove cellular debris. Clarified lysates were incubated with Protein A-Sepharose beads (Amersham Biosciences, Tokyo, Japan), which had been coupled with anti-c-myc antibody (Roche Pharmaceuticals), for 3 h rotating at 4°C. The beads were collected and washed with TS buffer three times, and the immunoprecipitates were separated from the beads by added 1mg/ml c-Myc peptide (SIGMA, Tokyo, Japan) solution to beads and incubated for 30 minutes at 4°C. And then supernatant were collected and boiling for 10 min in 1x protein sample buffer (100 mM Tris-HCl, pH 6.8, 4% [v/v] SDS, 10% [v/v] sucrose, 10% [v/v] β-mercaptoethanol). Samples were analyzed using SDS–polyacrylamide gel electrophoresis (PAGE) and subsequent immunoblotting with appropriate primary and secondary antibodies. Signals were visualized by chemiluminescence using ECL Plus Western Detection System (Ge Healthcare, Tokyo, Japan).

Isolation of mutant plants.

T-DNA insertion line (SALK_017580) was used as a mutant defective in *AtRPA70a*. After self-pollination three times, homozygous mutant line was identified by PCR-based genotyping with a REDExtract-N-Amp Plant PCR Kit (Sigma-Aldrich, St. Louis, MO, USA) using the forward primer F1 (5'-ATGCCGGTGAGTTTGACTCCG-3') and reverse primer R2 (5'-AATAGGGATGACTCGAGCTGG-3'), or using F1, R2 and T-DNA-specific primer LBa1 (5'-TGGTTCACGTAGTGGGCCATCG-3'). Accumulation of *AtRPA70a* transcript in rosette leaves of mutant lines was analyzed by RT-PCR using primers F1 and R3 (5'-GCCTTTAACGTCGCTACAAATG-3') or F2 (5'-CAGCTTGTCCTTTGATGATCGG-3') and R1 (5'-TTACCTTACGAGCAAATCAAG-3'). For control experiments, *AtUBQ1* was amplified as described above. To create *atrapa70a* and *attert* double mutant, pistils of *atrpa70a* T1 line were crossed with pollens of *attert* G4 line to yield F1 progeny. To identify the double mutant line, segregating progenies in F2 were genotyped as described above using AtTERT-specific primers AtTERT_F1 (5'-ATAGTTGGCGAGGATGTAGACC-3') and AtTERT_R1 (5'-CTTCAACACTGGGACATTTGGG-3').

Plant transformation.

For functional complementation of *atrpa70a*, a 4.3 kb genomic DNA fragment containing the *AtRPA70a* coding

region, 1.5 kb upstream region and 0.5 kb downstream region was amplified by PCR with the primers gAR70aF (5'-GAATCTAGATGCAGTCGACTCTGTCAGCTG-3'; *Xba*I site is underlined) and gAR70aR (5'-CTTGAGCTCGCACAGAGGCTTCAAGTTAAG-3'; *Sac*I site is underlined). The amplified fragment was cloned in *Xba*I and *Sac*I site of *Agrobacterium* binary vector pBIG-HYG (Becker, 1990) to yield a construct named pBIG-gAR70a. To generate *Arabidopsis* plants that express *AtTERT* antisense RNA, we amplified the full-length *AtTERT* ORF (Oguchi et al., 1999) by PCR with the primers ATASf (5'-GCTCTAGATCAATAATTCAACTTCCACAG-3'; *Xba*I site is underlined) and ATASr (5'-GCGAGCTCATGCCGCGTAAACCTAGACAT-3'; *Sac*I site is underlined). The amplified fragment was digested with *Xba*I and *Sac*I and was cloned into the pBIG-HYG, in which a *Hin*dIII-*Xba*I fragment of cauliflower mosaic virus (CaMV) 35S promoter had been subcloned from pBI121 (Clontech), to yield a construct (pBIG-ATas) containing *AtTERT* in the antisense orientation downstream of the plant specific promoter. The pBIG-gAR70a and pBIG-ATas vectors were transferred from *E. coli* to *A. tumefaciens* C58 by triparental mating with the use of the helper plasmid pRK2013 (Clontech), and the latter bacteria were then used to transform *atrpa70a* mutant plants by vacuum infiltration (Bechtold and Pelletier, 1998). Transformed seeds (T1 generation) were selected on MS medium containing 1% (w/v) sucrose and hygromycin B (20 μg/ml), and hygromycin-resistant T1 seedlings were transferred to soil and grown to maturity. The resulting T2 seed populations were screened for hygromycin resistance and the resistant plants were used for analyses.

Telomere length measurement.

Genomic DNA was extracted from rosette leaves of four-week-old *Arabidopsis* plant lines with the use of a NucleoSpin Plant L kit (Macherey-Nagel Inc., PA, USA). Terminal restriction fragment (TRF) analysis was performed as described previously (Zhang et al., 2006). Briefly, the DNA (10 μg) was digested with *Tru*9I and subjected to Southern hybridization with a DIG-labeled probe $(TTTAGGG)_4$ for telomeric repeats. Hybridization was detected with a chemiluminescence system (Roche).

Acknowledgments

We thank the RIKEN Biological Resource Center and the Salk Institute Genomic Analysis Laboratory for providing the *Arabidopsis* suspension cultured cells (T87 line) and the sequence-indexed *Arabidopsis* T-DNA insertion mutants (SALK 017580), respectively. We are grateful to Dr. Dorothy Shippen (Texas A & M University, USA) for providing the *attert* mutant line. This work was supported in part by Grant-in-Aid for Scientific Research (C) 17580037 from the Ministry of Education, Science, Sports and Culture of Japan.

References

Ball, H.L., Myers, J.S., and Cortez, D. (2005) ATRIP binding to replication protein A-single-stranded DNA promotes ATR-ATRIP localization but is dispensable for Chk1 phosphorylation. Mol. Biol. Cell 16, 2372–2381.

Bechtold, N., and Pelletier, G. (1998) *In planta Agrobacterium*-mediated transformation of adult *Arabidopsis thaliana* plants by vacuum infiltration. Methods Mol. Biol. 82, 259–266.

Becker, D. (1990) Binary vectors which allow the exchange of plant selectable markers and reporter genes. Nucleic Acids Res. 18, 203.

Binz, S.K., Sheehan, A.M., and Wold, M.S. (2004) Replication protein A phosphorylation and the cellular response to DNA damage. DNA Repair 3, 1015–1024.

Bochkareva, E., Belegu, V., Korolev, S. and Bochkarev, A. (2001) Structure of the major single stranded DNA-binding domain of Replication Protein A suggests a dynamic mechanism for DNA binding. EMBO J. 20, 612–618.

Bochkareva, E., Korolev, S., and Bochkarev, A. (2000) The role for zinc in replication protein A. J. Biol. Chem. 275, 27332–27338.

Braun, K.A., Lao, Y., He, Z., Ingles, C.J. and Wold, M.S. (1997) Role of protein-protein interactions in the function of replication protein A (RPA): RPA modulates the activity of DNA polymerase alpha by multiple mechanisms. Biochemistry, 36, 8443–8454.

Bundock, P., and Hooykaas, P. (2002) Severe developmental defects, hypersensitivity to DNA-damaging agents, and lengthened telomeres in Arabidopsis *MRE11* mutants. *Plant Cell* 14, 2451–2462

Bullock, P.A. (1997) The initiation of simian virus 40 DNA replication *in vitro*. Crit. Rev. Biochem. Mol. Biol. 32, 503–568.

Cahill, D., Connor, B. and Carney, J.P. (2006) Mechanisms of eukaryotic DNA double strand break repair. Front. Biosci. 11, 1958–1976.

Cohen, S., Jacob, E., and Manor, H. (2004) Effects of single-stranded DNA binding proteins on primer extension by telomerase. Biochim. Biophys. Acta 1679, 129–140.

Daniely, Y., and Borowiec, J.A. (2000) Formation of a complex between nucleolin and replication protein A after cell stress prevents initiation of DNA replication. J. Cell Biol. 149, 799–810.

Doherty, K.M., Sommers, J.A., Gray, M.D., Lee, J.W., von Kobbe, C., Thoma, N.H., Kureekattil, R.P., Kenny, M.K. and Brosh, R.M., Jr (2005) Physical and functional mapping of the replication protein A interaction domain of the Werner and Bloom syndrome helicases. J. Biol. Chem. 280, 29494–29505.

Fanning, E., Klimovich, V., and Nager, A.R. (2006) A dynamic model for replication protein A (RPA) function in DNA processing pathways. Nucleic Acids Res. 34, 4126–4137.

Fields, S. and Sternglanz, R. (1994) The two-hybrid system: an assay for protein–protein interactions. Trends Genet. 10, 286–292.

Fitzgerald, M.S., Riha, K., Gao, F., Ren, S., McKnight, T.D., and Shippen, D.E. (1999) Disruption of the telomerase catalytic subunit gene from *Arabidopsis* inactivates telomerase and leads to a slow loss of telomeric DNA. Proc. Natl. Acad. Sci. USA 96, 14813–14818.

Frank-Vaillant, M., and Marcand, S. (2002) Transient stability of DNA ends allows nonhomologous end joining to precede homologous recombination. Mol. Cell 10, 1189-1199.

Gallego, M.E., Jalut, N., and White, C.I. (2002) Telomerase dependence of telomere lengthening in *ku80* mutant Arabidopsis. Plant Cell 15, 782–789.

Gallego, M.E. and White, C.I. (2001) RAD50 function is essential for telomere maintenance in *Arabidopsis.* Proc. Natl. Acad. Sci. USA 98, 1711–1716.

Garcia-Maya, M.M., and Buck, K.W. (1997) Isolation and characterization of replication protein A (RPA) from tobacco cells. FEBS Lett. 413, 181–184.

Grandin, N., and Charbonneau, M. (2007) Control of the yeast telomeric senescence survival pathways of recombination by the Mec1 and Mec3 DNA damage sensors and RPA. Nucleic Acids Res. 35, 822–838.

Henson, J.D., Neumann, A.A., Yeager, T.R., and Reddle, R.R. (2001) Alternative lengthening of telomeres in mammalian cells. Oncogene 21, 598–610.

Ishibashi, T., Kimura, S., Furukawa, T., Hatanaka, M., Hashimoto, J., and Sakaguchi, K. (2001). Two types of replication protein A 70 kDa subunit in rice, Oryza sativa: Molecular cloning, characterization, and cellular & tissue distribution. Gene 272, 335–343.

Ishibashi, T., Koga, A., Yamamoto, T., Uchiyama, Y., Mori, Y., Hashimoto, J., Kimura, S., and Sakaguchi, K. (2005). Two types of replication protein A in seed plants. FEBS J. 272, 3270–3281.

Iftode, C., Daniely, Y. and Borowiec, J.A. (1999) Replication Protein A (RPA): the eukaryotic SSB. Crit. Rev. Biochem. Mol. Biol. 34, 141–180.

Keshav, K.F., Chen, C., and Dutta, A. (1995) Rpa4, a homolog of the 34-kilodalton subunit of the replication protein A complex. Mol. Cell. Biol. 15, 3119–3128.

Kim, K., Dimitrova, D.D., Carta, K.M., Saxena, A., Daras, M., and Borowiec, J.A. (2005) Novel checkpoint response to genotoxic stress mediated by nucleolin-replication protein A complex formation. Mol. Cell. Biol. 25,

2463–2474.

Kim, C., Paulus, B.F., and Wold, M.S. (1994) Interactions of human replication protein A with oligonucleotides. Biochemistry 33, 14197–14206.

Longhese, M.P., Neecke, H., Paciotti, V., Lucchini, G., and Plevani, P. (1996) The 70 kDa subunit of replication protein A is required for the G1/S and intra-S DNA damage checkpoints in budding yeast. Nucleic Acids Res. 24, 3533–3537.

Lundblad, V. (2002) Telomere maintenance without telomerase. Oncogene 21, 522–531.

Namiki, Y., and Zou, L. (2006) ATRIP associates with replication protein A-coated ssDNA through multiple interactions. Proc. Natl Acad. Sci. USA 103, 580–585.

Oguchi, K., Liu, H., Tamura, K., and Takahashi, H. (1999) Molecular cloning and characterization of AtTERT, a telomerase reverse transcriptase homolog in *Arabidopsis thaliana*. FEBS Lett. 457, 465–469.

Ono, Y., Tomita, K., Matsuura, A., Nakagawa, T., Masukata, H., Uritani, M., Ushimaru, T. and Ueno, M. (2003) A novel allele of fission yeast rad11 that causes defects in DNA repair and telomere length regulation. Nucleic Acids Res. 31, 7141–7149.

Opresko, P.L., von Kobbe, C., Laine, J.P., Harrigan, J., Hickson, I.D., and Bohr, V.A. (2002) Telomere-binding protein TRF2 binds to and stimulates the Werner and Bloom syndrome helicases, J. Biol. Chem. 277, 41110–41119.

Pacher, M., Schmidt-Puchta, W., and Puchta, H. (2007) Two unlinked double-strand breaks can induce reciprocal exchanges in plant genomes via homologous recombination and nonhomologous end joining. Genetics 175, 21–29.

Riha, K., Watson, J.M., Parkey, J., and Shippen, D.E. (2001) Telomere length deregulation and enhanced sensitivity to genotoxic stress in *Arabidopsis* mutants deficient in Ku70. EMBO J. 21, 2819–2826.

Robison, J.G., Elliott, J., Dixon, K., and Oakley, G.G. (2004) Replication protein A and the Mre11.Rad50.Nbs1 complex co-localize and interact at sites of stalled replication forks. J. Biol. Chem. 279, 34802–34810.

Salas, T.R., Petruseva, I., Lavrik, O., Bourdoncle, A., Mergny, J.L., Favre, A., and Saintome, C. (2006) Human replication protein A unfolds telomeric G-quadruplexes. Nucleic Acids Res. 34, 4857–4865.

Sambrook, J., Fritsch, E.F., and Maniatis, T. (1989) Molecular Cloning: A Laboratory Manual, 2nd edn. Cold Spring Harbor, NY: Cold Spring Harbor Laboratory Press.

Schramke, V., Luciano, P., Brevet, V., Guillot, S., Corda, Y., Longhese, M.P., Gilson, E., and Géli, V. (2004) RPA regulates telomerase action by providing Est1p access to chromosome ends. Nat. Genet. 36, 46–54.

Smith, J., Zou, H., and Rothstein, R. (2000) Characterization of genetic interactions with *RFA1*: the role of RPA in DNA replication and telomere maintenance. Biochimie 82, 71–78.

Sogo, J.M., Lopes, M., and Foiani, M. (2002) Fork reversal and ssDNA accumulation at stalled replication forks owing to checkpoint defects. Science 297, 599–602.

Song, B., and Sung, P. (2000) Functional interactions among yeast Rad51 recombinase, Rad52 mediator, and replication protein A in DNA strand exchange. J. Biol. Chem. 275, 15895–15904.

Stenlund, A. (2003) Initiation of DNA replication: lessons from viral initiator proteins. Nat. Rev. Mol. Cell Biol. 4, 777–785.

Sugiyama, T., and Kowalczykowski, S.C. (2002) Rad52 protein associates with replication protein A (RPA)-single-stranded DNA to accelerate Rad51-mediated displacement of RPA and presynaptic complex formation. J. Biol. Chem. 277, 31663–31672.

Symington, L.S. (2002) Role of RAD52 epistasis group genes in homologous recombination and double-strand break repair. Microbiol. Mol. Biol. Rev. 66, 630–670.

Tamura, K., Adachi, Y., Chiba, K., Oguchi, K., and Takahashi, H. (2002) Identification of Ku70 and Ku80 homologues in *Arabidopsis thaliana*: evidence for a role in the repair of DNA doublestrand breaks. Plant J. 29, 771–781.

Tamura, K., Dudley, J., Nei, M. and Kumar, S. (2007) Molecular Evolutionary Genetics Analysis (MEGA) Software Version 4.0 Mol. Biol. Evol. 24, 1596-1599.

Thompson, J.D., Higgins, D.G., and Gibson, T.J. (1994) CLUSTAL W: improving the sensitivity of progressive multiple sequence alignment through sequence weighting, position-specific gap penalties and weight matrix choice. Nucleic Acids Res. 22, 4673–4680.

Tuteja, N., Singh, M.B., Misra, M.K., Bhalla, P.L., and Tuteja, R. (2001) Molecular mechanisms of DNA damage and repair: progress in plants. Crit. Rev. Biochem. Mol. Biol. 36, 337–397.

van der Knaap, E., Jagoueix, S., and Kende, H. (1997) Expression of an ortholog of replication protein A1 (RPA1) is induced by gibberellin in deepwater rice. Proc. Natl. Acad. Sci. USA 94, 9979–9983.

Verdun, R.E. and Karlseder, J. (2006) The DNA damage machinery and homologous recombination pathway act consecutively to protect human telomeres. Cell 127, 709–720.

Viscardi, V., Clerici, M., Cartagena-Lirola, H., and Longhese, M.P. (2005) Telomeres and DNA damage checkpoints. Biochimie 87, 613–624.

Wold, M.S. (1997) Replication Protein A: a heterotrimeric, single-stranded DNA-binding protein required for eukaryotic DNA metabolism. Annu. Rev. Biochem. 66, 61–92.

Wong, J.M.S., Ionescu, D., and Ingles, C.J. (2003) Interaction between BRCA2 and replication protein A is compromised by a cancer-predisposing mutation in BRCA2. Oncogene 22, 28–33.

Wu, X., Shell, S.M. and Zou, Y. (2005) Interaction and colocalization of Rad9//Rad1//Hus1 checkpoint complex with replication protein A in human cells. Oncogene 24, 4728–4735.

Xia, R., Wang, J., Liu, C., Wang, Y., Wang, Y., Zhai, J., Liu, J., Hong, X., Cao, X., Zhu, J.-K., and Gonga, Z. (2006) ROR1/RPA2A, a putative replication protein A2, functions in epigenetic gene silencing and in regulation of meristem development in Arabidopsis. Plant Cell 18, 85–103.

Yoo, E., Kim, B.U., Lee, S.Y., Cho, C.H., Chung, J.H. and Lee, C.-H. (2005) 53BP1 is associated with replication protein A and is required for RPA2 hyperphosphorylation following DNA damage. Oncogene 24, 5423–5430.

Zaug, A.J., Podell, E.R., and Cech, T.R. (2005) Human POT1 disrupts telomeric G-quadruplexes allowing telomerase extension in vitro, Proc. Natl. Acad. Sci. USA 102, 10864–10869.

Zhang, L., Tamura, K., Shin-ya, K., and Takahashi, T. (2006) The telomerase inhibitor telomestatin induces telomere shortening and cell death in *Arabidopsis*. Biochim. Biophys. Acta 1763, 39–44.

Zou, L. and Elledge, S.J. (2003) Sensing DNA damage through ATRIP recognition of RPA-ssDNA complexes. Science 300, 1542–1548.

Zou, L., Liu, D., and Elledge, S.J. (2003) Replication protein A-mediated recruitment and activation of Rad17 complexes. Proc. Natl. Acad. Sci. USA 100, 13827–13832.

Table 1. Similarity of amino acid sequence of conserved domains in pairwise comparison among AtRPA70a, AtRPA70b, AtRPA70c, AtRPA70d and HsRPA1

Rep-A_N *				
	AtRPA70a	AtRPA70b	AtRPA70c	AtRPA70d
AtRPA70a				
AtRPA70b	22.33			
AtRPA70c	34.58	26.79		
AtRPA70d	24.51	74.51	28.57	
HsRPA1	38.10	17.92	33.64	16.67
tRNA_anti *				
	AtRPA70a	AtRPA70b	AtRPA70c	AtRPA70d
AtRPA70a				
AtRPA70b	50.55			
AtRPA70c	68.13	47.25		
AtRPA70d	47.25	94.51	49.45	
HsRPA1	51.09	56.04	48.35	54.95
Rep_fac-A_C*				
	AtRPA70a	AtRPA70b	AtRPA70c	AtRPA70d
AtRPA70a				
AtRPA70b	31.37			
AtRPA70c	61.84	30.07		
AtRPA70d	30.07	83.67	28.10	
HsRPA1	30.92	32.21	36.18	34.23

Each value indicates percentage of similarity.

* Domain names are same as in Fig. 1A.

Figure Legends

Figure 1. Domain structures of *Arabidopsis* RPA70 paralogs and their phylogenetic relationship.

A, Structures of AtRPA70 paralogs. Rep-A_N, Replication factor-A protein 1, N-terminal domain; tRNA_anti, the anti-codon binding domain of lysyl, aspartyl, and asparaginyl–tRNA synthetases; Rep_fac-A_C, Replication factor-A protein 1, C-terminal domain. Rep-A_N and tRNA_anti contain DNA-binding domains (DBDs). The number of amino acid residues of each paralog is shown in parenthesis followed by E-value against *Homo sapiens* RPA1. B, Phylogenetic relations among RPA homologues. The number at each node indicates the percentage of 1000 bootstrap replicates required for statistical significance. GenBank accession numbers are as follows (organisms in parentheses): HsRPA1 (*Homo sapiens*), M63488; ScRPA1 (*Saccharomyces cerevisiae*), X59748; SpRAD11 (*Schizosaccharomyces pombe*), U59385; DmRPA1 (*Drosophila melanogaster*), Z70277; MmRPA1 (*Mus musculus*), BC019119; XlRPA1 (*Xenopus laevis*), BC070559; OsRPA1 (*Oryza sativa*), AF009179; OsRPA70a, AB042415; OsRPA70b, AB111916; OsRPA70c, AK073598.

Figure 2. *AtRPA70a* expresses ubiquitously in plant organs and is upregulated by genotoxic stress.

A, Steady-state mRNA levels of *AtRPA70a* in various plant organs and cultured cells. Total RNA was extracted from indicated organs of *Arabidopsis* mature plant and one-week-old seedlings as well as cultured cells (T87 line). The RNAs were separated on a 1.3% agarose gel containing formaldehyde and were subjected to hybridization with DIG-labeled 3'UTR of *AtRPR70a* used as the probe. B, Expression of *AtRPA70a* in response to DNA damaging agents. One-week-old *Arabidopsis* seedlings were treated with methylmethane sulfonate (MMS) or bleomycin in liquid MS medium. After the incubation with shaking for the indicated times (h), total RNA was isolated and analyzed same as in *A*. Similar amounts of RNAs were loaded in each lane as confirmed by ethidium bromide staining (lower panel). The experiments were repeated three times with similar results.

Figure 3. AtRPA70a interacts more strongly with AtRPA32a than AtRPA32b.

A, Yeast two-hybrid interaction between AtRPA70a and AtRPA32 paralogs. Growth of transformed yeast strains on SD agar media without tryptophan, leucine, uracil, histidine and adenine (-L, W, U, H, A) (or supplemented with 10 mM 3-AT) were assayed for reporter yeast cells. Growth on SD agar media lacking tryptophan, leucine and uracil (-L, W, U) were used as control. B, Liquid β-galactosidase assay. The enzyme activity in yeast transformants was measured using ONPG (o-nitrophenyl β-D-galactopyranoside) as the substrate. C, Co-immunoprecipitation assay. c-Myc-tagged AtRPA32a (Myc-32a) and AtRPA32b (Myc-32b) or c-Myc alone were immunoprecipitated using anti-c-Myc antibody, and HA-tagged AtRPA70a (HA-70a) was detected from the immunoprecipitates by protein gel blot analysis with anti-HA antibody (upper panel). Similar amounts of total proteins were loaded in each lane as confirmed by Commassie Brilliant Blue staining (lower panel).

Figure 4. *AtRPA70a*-deficient mutant plants are hypersensitive to genotoxic stress.

A, Genomic organization of *AtRPA70a* and T-DNA insertion site. The gray and white boxes indicate the open reading fame consisting of separated exons and 5' untranslated region, respectively. The horizontal and vertical bars represent the location of intron and the position of T-DNA insertion in SALK_017580 line. The arrows

indicate the positions of primers used in *B*, *C*. B, Genomic PCR verifying the insertion of T-DNA in *AtRPA70a*. +/- and -/- indicate heterozygous and homozygous *atrpa70a* lines, respectively. Upper and middle rows indicate *AtRPA70a*, and lower row indicates *AtUBQ1*. *AtUBQ1* gene was used to normalize the efficiency of PCR. C, Detection of *AtRPA70a* transcript by RT-PCR. *AtUBQ1* gene was also amplified to normalize both the amount of input RNA for the RT reaction and the efficiency of PCR. D, Sensitivity to genotoxic stress. One-week-old seedlings of Col-0 and *atrpa70a* mutant were transplanted onto MS agar medium containing MMS, bleomycin, or hydroxyurea (HU) at the concentrations indicated, and photos were taken after 7 days of incubation. E, Root length of Col-0 and *atrpa70a* mutant in *D*. Data are presented as mean ± SD (n=8). The asterisk indicates significant difference between Col-0 and *atrpa70a* mutant at the dose ($p < 0.01$).

Figure 5. Telomere lengthening in *atrpa70a* plant.

Telomere lengths were analyzed by the TRF assay. Genomic DNA was isolated from rosette leaves of four-week-old Col-0 (lanes 1, 8), *atrpa70a* (lanes 2, 3, 9, 10, 13), *atrpa70a attert* G4 double mutant line (lanes 4, 5), *attert* G4 (lanes 6, 7), *atrpa70a* lines transformed with genomic *AtRPA70a* (lanes 11, 12), and *atrpa70a* lines expressing antisense *AtTERT* (lanes 14-16). DIG-labeled $(TTTAGGG)_4$ was used as the probe for determination of telomere length. Results are shown for two siblings or three independent lines with the expression of antisense *AtTERT*. Signals corresponding to telomeric or interstitial telomeric sequences are indicated by single and double arrowheads, respectively. The dashed bar represents the mean telomere length of Col-0. Lanes M contain *Hin*dIII-digested phage λ DNA; fragment size is indicated in kilobases.

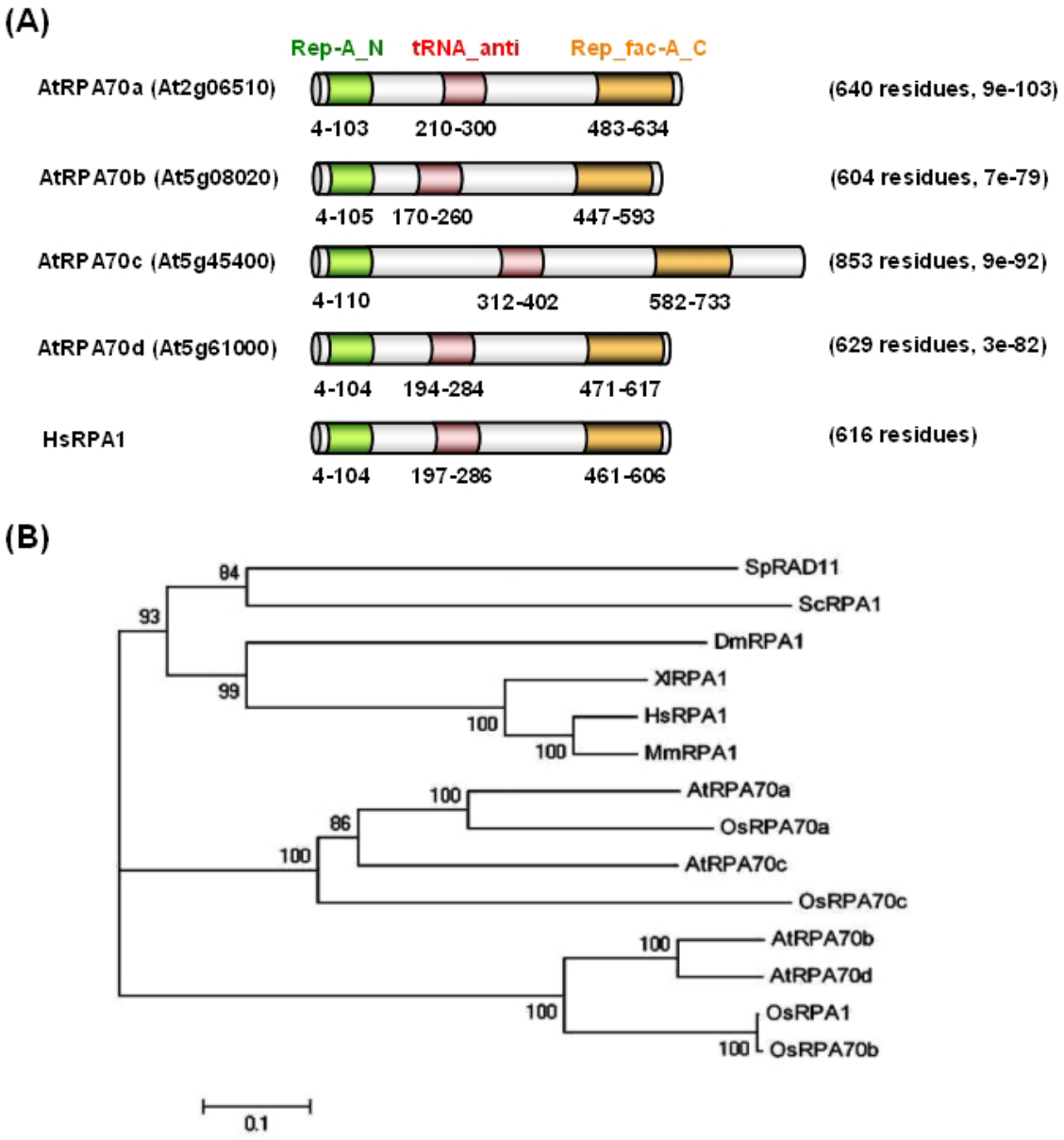

Fig. 1

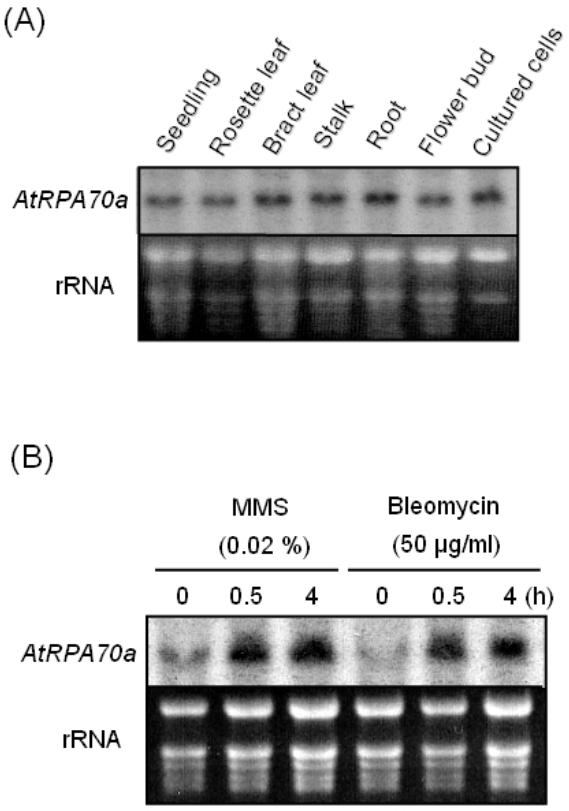

Fig. 2

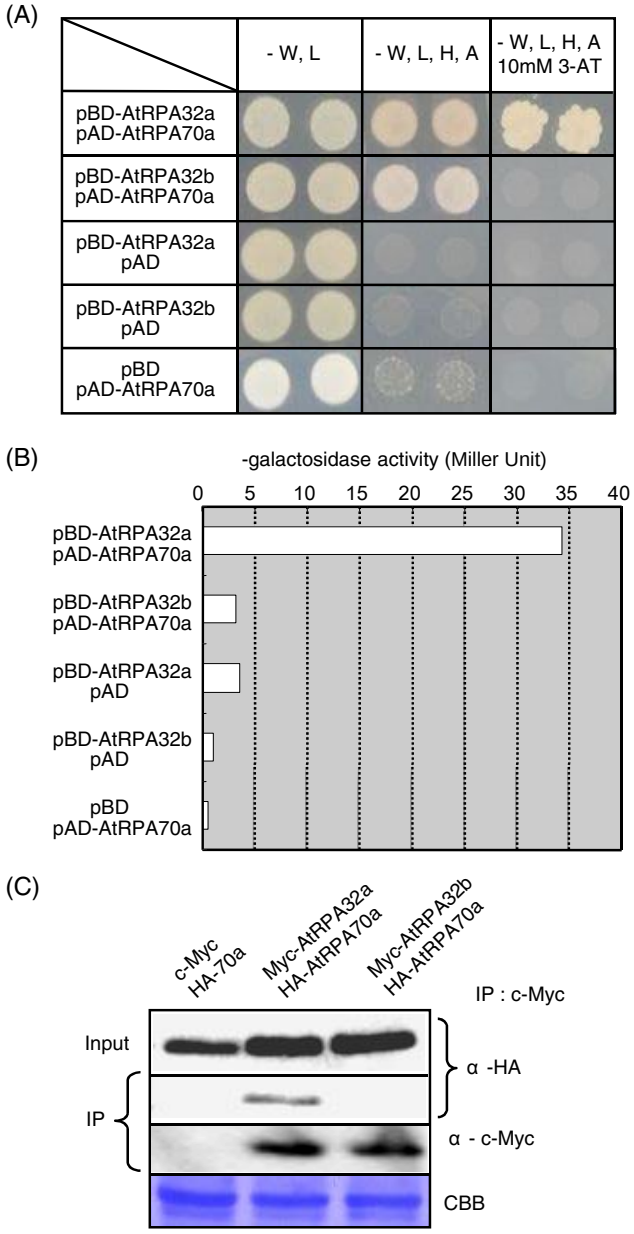

Fig. 3

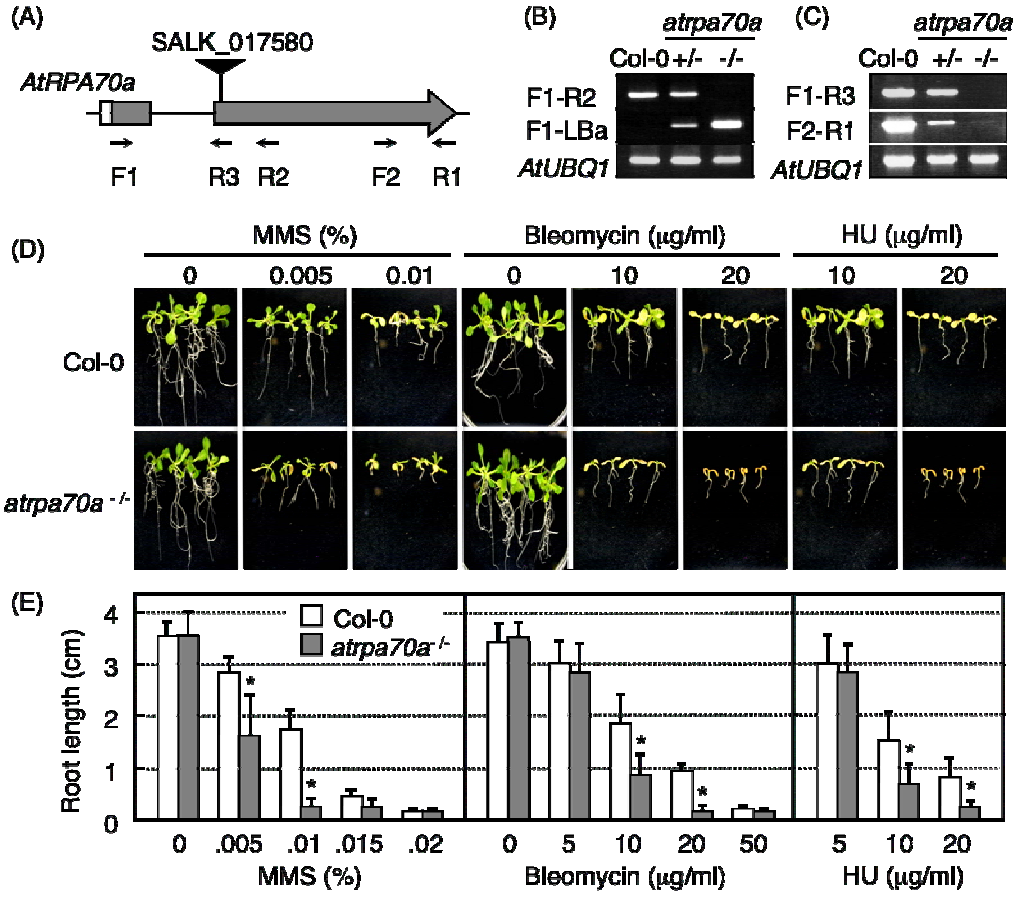

Fig. 4

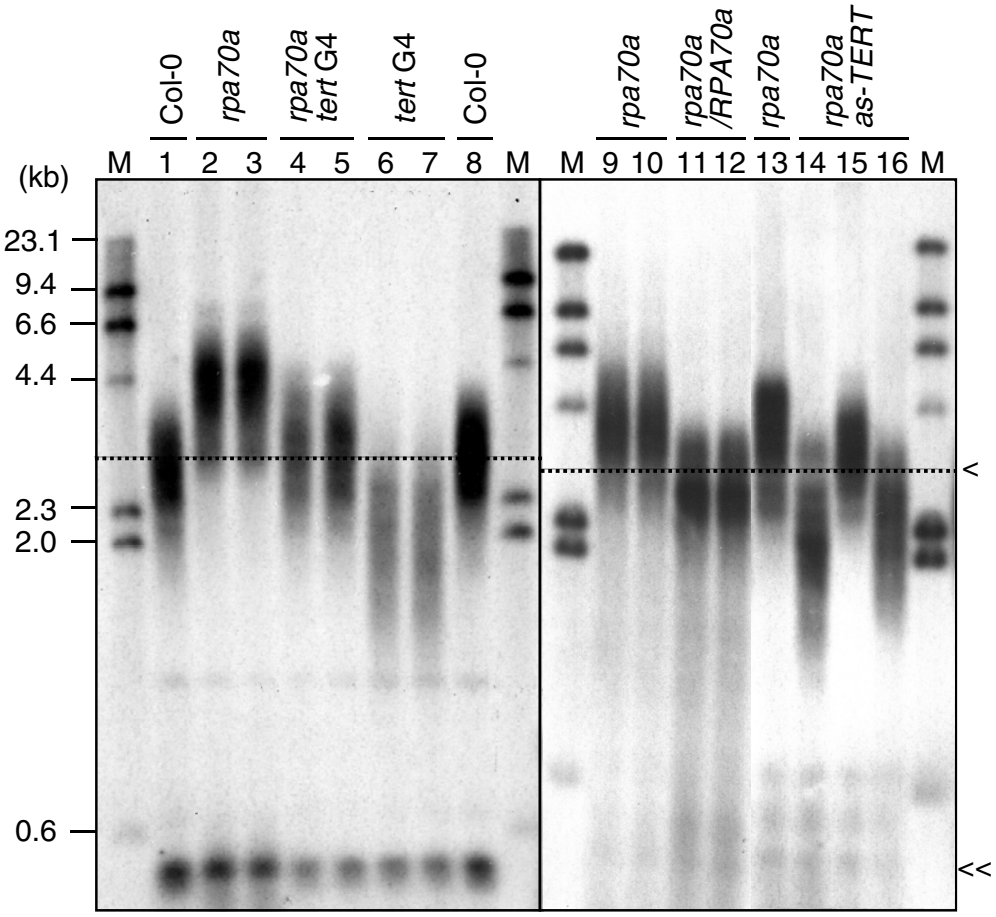

Fig. 5